Article

Investigating the Sorption/Desorption of the Cationic Herbicide Paraquat in Clay Minerals Using Batch and Electro–Ultrafiltration Techniques

Stefano Salvestrini *, Eleonora Grilli and Elio Coppola

Department of Environmental, Biological and Pharmaceutical Sciences and Technologies, University of Campania "Luigi Vanvitelli", Via Vivaldi 43, 81100 Caserta, Italy; eleonora.grilli@unicampania.it (E.G.); elio.coppola@unicampania.it (E.C.)
* Correspondence: stefano.salvestrini@unicampania.it

Abstract: The sorption/desorption processes of the cationic herbicide paraquat (PQ) onto various clays, namely, kaolinite (KLN), illite (ILT), and montmorillonite (MNT), were investigated. After the attainment of sorption equilibrium, PQ was extracted from the clays by a double-stage desorption process utilizing an electro–ultrafiltration (EUF) procedure. The Freundlich isotherm model and a pseudo-first kinetic release model were found to adequately fit the sorption and desorption data, respectively. The experimental maximum sorbable amounts of paraquat were 5.56, 31.88, and 91.63 mg g^{-1} for KLN, ILT, and MNT, respectively, consistently with the order of magnitude of the cation-exchange capacity (CEC) of the clay minerals. The desorption experiments revealed that the amounts of PQ retained by the MNT samples were significantly larger than the respective amounts retained by KLN or ILT. The EUF-PQ desorption patterns of differently cation-saturated MNT samples indicated that the presence of monovalent cations could further hamper PQ release, while the opposite seemed to be true for divalent cations. Our results clearly show that a substantial aliquot of PQ is strongly retained by montmorillonite, probably via interlayering, thus suggesting that smectitic clays could act as a stable soil sink for cationic herbicides such as paraquat, favoring soil long-term contamination.

Keywords: clay minerals; paraquat; electro–ultrafiltration; sorption; desorption

1. Introduction

The compound 1,1′-dimethyl-4,4′-bipyridinium dichloride, commonly known as paraquat (PQ), is a nonselective foliar herbicide that has been used in more than 100 countries, among which the U.S.A. and Brazil [1], for more than 60 years. Despite PQ being excessively toxic to all living organisms including humans [2,3], its unique properties, i.e., rapid action, limited mobility in the soil environment, and hence, reduced effect on roots and rhizomes, have enabled its widespread use [4], including in sustainable farming systems [5]. Indeed, as many herbicides, PQ exhibits a high affinity for soil components, in particular humic substances and clay minerals, by which it is strongly sorbed, becoming protected against leaching and microbial degradation and remaining inactivated for a long time period [6–8]. With reference to clay minerals, the literature data clearly show that the PQ sorption mechanism is complex, mainly governed by cation-exchange interactions and enhanced by additional processes such as interlayer sorption into expanding lattice minerals, H- bridging, van der Waals interactions, and charge transfer [9–11]. The capacity of a soil to sorb PQ strongly depends on the amount and type of clay minerals it contains: non-expandable kaolinite is capable of sorbing, in total, about 2500–3000 mg kg^{-1} of PQ, while expandable montmorillonite can sorb up to 75,000–85,000 mg kg^{-1} [5]. Furthermore, clay minerals' features also control PQ mobility in the soil environment, as PQ remains

exchangeable and hence available to living organisms if sorbed on kaolinite and vermiculite but not if bound to montmorillonite or smectite [12,13].

Under normal application conditions, most paraquat (some 99.99%) is strongly sorbed to soil [5,14], with just a small amount of it remaining in solution in the soil and constituting the potentially bioavailable fraction. PQ loosely bound to soil components could be available for living organisms as a result of desorption processes [15]. This free PQ can be taken up by crop roots, as discovered by several studies in field and greenhouse conditions [15–17] as well as in laboratory conditions [18,19]. Therefore, to better predict the fate of clay mineral-bound paraquat in soil, it is useful to investigate not only its sorption mechanism but also the kinetics of its release [20–22].

A useful technique to obtain both quantitative and kinetics information on nutrient availability is electro–ultrafiltration (EUF), introduced by Németh [23] as a multiple-element soil test to determine nutrient availability to plants. Over the years, the application of this technique has been extended, for example, to the modelling of plant uptake of metals [24], the reduction of membrane fouling in industrial processes [25–27], and the removal of heavy metals from water [28]. EUF involves a combination of electrodialysis and ultrafiltration to remove electrolytes from aqueous suspensions under controlled electrical field strength and temperature [29,30]. By the suitable adjustment of electrical field strength and temperature, the fractions of a given compound retained with different energy levels by a soil matrix can be collected. Under low-energy extraction conditions, the loosely bound, easily exchangeable forms of the compound are prevailingly extracted. In high-energy conditions, the strongly retained and part of the selectively retained exchangeable forms of the compound are also extracted [31,32].

By performing stepwise extractions, the EUF technique allows for estimating both the actual as well as the potential supply of a compound and for obtaining its release kinetic parameters [29,30]. Moreover, EUF offers some advantages compared with classical ion-exchange techniques, as follows: (1) the use of pure water as the reaction medium avoids undesired side effects due to foreign electrolytes; (2) the solution is continuously diluted under a constant soil/suspension ratio, preventing the aggregation of soil particles; (3) element release is not mediated by a specific ion-exchange reaction but is essentially dependent on the strength of element/matrix interactions. All this makes the performance of EUF in providing extraction isotherms free from the constraints of the electrolytic nature of the medium and of ion selectivity and competition during the release process in exchange reactions.

On this basis, a study was carried out aiming at investigating by a batch method and the EUF technique the sorption and desorption of PQ in the presence of some clay minerals, i.e., kaolinite, illite, and montmorillonite. In addition, the effect of different saturating cations on PQ release from montmorillonite was also evaluated.

2. Materials and Methods

2.1. Clay Minerals

The clay minerals used in this study were kaolinite (KLN) from Macon (GA, USA), illite No. 35 (ILT) from Fithian (IL, USA), supplied by Ward's Natural Science Establishment Inc. (Rochester, NY, USA), and montmorillonite (MNT) from the Uri pit (Sardinia, Italy). The clays were preliminary treated once with 0.1 M HCl and five times with Na acetate buffer at pH 5.0, to remove alkaline and alkaline earth carbonates. Fractions with material <2 μm in size were collected by centrifugation and treated with a 1 M NaCl solution. The above procedure (centrifugation and NaCl treatment) was repeated on the collected clay fractions another four times to ensure Na^+ saturation. The excess salt was removed by washing the minerals with water for three times, then with water/acetone 1:1 until they were Cl^--free, and lastly with methanol to remove any impurities. Finally, the samples were dried in an oven at 40 °C for 3 days. The CECs of the Na-saturated clays were 6.7, 28.1, and 72.5 cmol [+] kg^{-1} for KLN, ILT, and MNT, respectively.

Oriented-aggregate specimens for X-ray powder diffraction (XRD) were obtained by drying aliquots of the samples (previously sonicated) on glass slides. The XRD patterns were recorded at room temperature with a Rigaku diffractometer using Fe-filtered Co Kα radiation.

2.2. Reagents

All reagents were purchased from Merck KGaA (Darmstadt, Germany). Because of its hygroscopic nature, PQ was stored in a desiccator over P_2O_5 until use.

2.3. Sorption Studies

2.3.1. Sorption Isotherms

The sorption experiments on PQ were conducted in 1.0 M NaCl. Preliminary tests showed that the ionic strength, in the investigated range of values, did not affect the PQ absorbance spectra. For each clay, a set of 1.0 M NaCl solutions containing PQ at a concentration ranging from 1.25 to 200.00 mg L^{-1} was prepared. The suspensions, prepared into stoppered 15 mL polypropylene centrifuge tubes, were shaken at 25.0 $\pm$ 0.5 °C for 16 h (a time sufficient for sorption equilibration) on a mechanical end-over-end shaker. Afterwards, the supernatant solutions were recovered by centrifugation at 15,000 rpm for 15 min and then analyzed for PQ spectrophotometrically, as explained in Section 2.5.

2.4. Desorption Studies

2.4.1. Addition of PQ to the Clays

Three sets of experiments were performed in three replicates, as follows:

(i) Clays containing an amount of PQ corresponding to their CEC value. We added 10 mL of aqueous solutions containing the suitable amount of PQ to 200 mg of KLN, ILT, or MNT into stoppered 100 mL polypropylene centrifuge tubes. The suspensions were kept under agitation as described for the sorption studies and then gently evaporated to dryness in an oven at 40 °C for 3 days, allowing the residual PQ in the liquid phase to deposit on the clays. The samples prepared in this way were denoted as KLN + PQCEC, ILT + PQCEC, and MNT + PQCEC, respectively.

(ii) Clays containing an amount of PQ in the ratios of 10:1 and 20:1 (*w:w*), roughly corresponding to the average PQ amount sorbable by KLT or MNT and the highest PQ amount sorbable by MNT in the sorption experiments (see Section 2.3.1), respectively. We added 10 mL of aqueous solutions containing 10 or 20 mg of PQ to 200 mg of each clay. The samples were then prepared as described above in (i) and hereafter denoted as KLN + PQ100, ILT + PQ100, and MNT + PQ100 or KLN + PQ50, ILT + PQ50, and MNT + PQ50, respectively.

(iii) Samples containing amounts of PQ corresponding to the CEC of MNT, in which MNT was saturated with K^+, NH_4^+, Ca^{2+}, or Mg^{2+} ions according to the procedure described for Na saturation (see Section 2.1). The samples were prepared as in (i) and henceforth are referred to as Na- K-, NH4-, Ca-, and Mg-MNT, respectively.

At the end of the experiments, the dried material was lightly ground in an agate mortar, passed through a 0.5 mm sieve, and finally subdivided in three subsamples again.

2.4.2. Desorption of PQ by EUF (EUF-PQ)

The EUF apparatus Vogel 724 (Giessen, Germany) was used for the extraction phase. Fifty milligrams of each subsample of clay was used for the EUF-PQ desorption studies. The experiment was performed in three replicates. Two subsequent sets of extraction with pure water as the extractant, namely, EUF 1 at low energy and EUF 2 at high energy, were performed. For each set, six fractions were stepwise collected every 5 min under the conditions reported in Table 1.

For each fraction, the anodic and the cathodic extracts were pooled together into a graduated flask and then diluted up to 100 mL.

Table 1. EUF operational conditions.

Stage	Temperature (°C)	Maximum Electric Field Strength (V)	Current Intensity (mA)	Extraction Time (min)
EUF 1	20	200	15	0–30
EUF 2	80	400	150	30–60

EUF 1 = first extraction step at low energy. EUF 2 = second extraction step at high energy.

2.5. Determination of PQ in Solution

The equilibrium PQ concentrations in the liquid phase for the sorption studies and the PQ concentrations in the EUF extracts were determined spectrophotometrically by reading the absorbance at 256 nm. The absorbance spectra were recorded by continuous scanning from 400 to 200 nm using a UV-1280 Shimadzu instrument (Kyoto, Japan).

2.6. Data modelling

The sorption isotherm data were fitted by the Langmuir model [33] (Equation (1)), the Freundlich model [34] (Equation (2)), and the Jovanović model [35,36] (Equation (3))

$$q_e = \frac{q_m K_L C_e}{1 + K_L C_e} \tag{1}$$

$$q_e = K_F C_e{}^N \tag{2}$$

$$q_e = q_m \left(1 - e^{-K_J C_e} \right) \tag{3}$$

where

q_e = amount of sorbate taken up per unit mass of sorbent at a given equilibrium concentration C_e in solution;

q_m = maximum amount of sorbate that may be bound;

K_L = equilibrium Langmuir constant;

K_F = Freundlich constant;

N = heterogeneity index of the Freundlich model;

K_J = Jovanović constant.

The EUF release kinetics were fitted by pseudo-first-order (PFO, Equation (4)) and pseudo-second-order (PSO, Equation (5)) kinetic models [37] and are here expressed in terms of S, which is the residual amount of PQ retained per mass of clay.

$$S_t = S_0 - R_m \left(1 - e^{-k_1 t} \right) \tag{4}$$

$$S_t = S_0 - \frac{R_m{}^2 k_2 t}{1 + R_m k_2 t} \tag{5}$$

where

S_t = residual sorbed amount of PQ per mass of clay at time t;

t = extraction time;

k_1 and k_2 = kinetic constants related to the EUF release rate of PQ;

S_0 = initial content of desorbable PQ;

R_m = maximum amount of PQ per mass of clay that can be released.

For each desorption experiment, the R_m and k parameters were calculated from the second-stage extraction, EUF 2, data.

3. Results

3.1. Sorption

The experimental equilibrium data of PQ sorption onto clays were interpolated by the Langmuir, Freundlich, and Jovanović models. The estimated sorption parameters are reported in Table 2. According to the values of the coefficient of determination R^2, the isotherm data were, overall, better described by the Freundlich model.

Table 2. Estimated isotherm parameters for the sorption of PQ onto clays.

Clay	Model	q_m (mg g^{-1})	K_L (L mg^{-1})	N	K_F (L^N mg^{1-N} g^{-1})	K_J (L mg^{-1})	R^2
MNT	Langmuir	95 ± 2	0.13 ± 0.02				0.9939
MNT	Freundlich			0.18 ± 0.02	40 ± 3		0.9925
MNT	Jovanović	87 ± 1				0.0081 ± 0.009	0.9915
ILT	Langmuir	33 ± 1	0.070 ± 0.010				0.9991
ILT	Freundlich			0.27 ± 0.01	8.1 ± 0.4		0.9998
ILT	Jovanović	28.9 ± 0.8				0.050 ± 0.007	0.9982
KLN	Langmuir	5.7 ± 0.2	0.24 ± 0.03				0.9998
KLN	Freundlich			0.25 ± 0.02	2.1 ± 0.1		0.9999
KLN	Jovanović	5.2 ± 0.2				0.16 ± 0.02	0.9997

This suggested that the clays exhibited an energetically heterogeneous distribution of sorption sites [38]. The results of the interpolation by the Freundlich isotherm are graphically displayed in Figure 1.
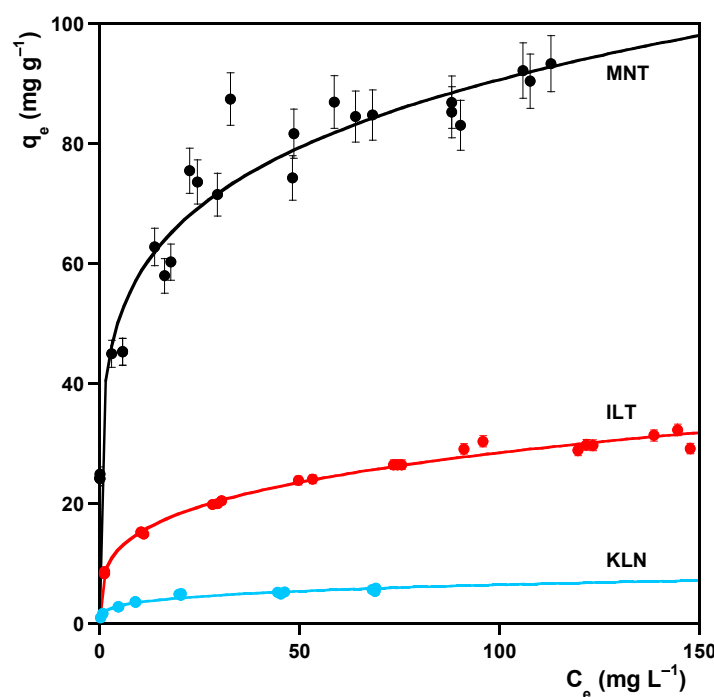
**Figure 1.** Sorption isotherms of PQ for the examined clays.

As can be seen in the figure, the investigated clay samples sorbed PQ in decreasing amounts in the order MNT > ILT > KLN. An average equilibrium constant (*K*) was estimated from the Freundlich isotherm using the expression [38]:

$$K = e^{\frac{1}{N}} \tag{6}$$

The K values for MNT, ILT, and KLN turned out to be 259 ± 160, 41 ± 6, and 55 ± 17, respectively. The results denoted that MNT not only exhibited a higher number of sorbing sites but also showed a greater affinity for PQ than kaolinite and illite, as inferred from the higher K value. Interestingly, the trend of the q_m values was consistent with that of the respective clay CECs.

3.2. Desorption

Figure 2 shows the cumulative EUF-PQ extracted from the Na-clay + PQ_{CEC} samples. To simplify the comparisons, the data are expressed as the percentage of residual PQ saturating the clay CEC. After completion of EUF 1, the amounts of PQ desorbed from KLN, ILT, and MNT were 4.4, 11.8, and 15.7 mg g^{-1}, respectively; after completion of EUF 2, further amounts of 1.73, 2.92, and 5.76 mg g^{-1} were released, so that the residual sorbed PQ, after 60 min of EUF extraction, was 45.9%, 59.2%, and 77.0% of the CECs of KLN, ILT, and MNT, respectively. The application of Equations (4) and (5) to the EUF-2 stage revealed that the pseudo-first-order kinetic release model better described the experimental desorption data (see Table 3).
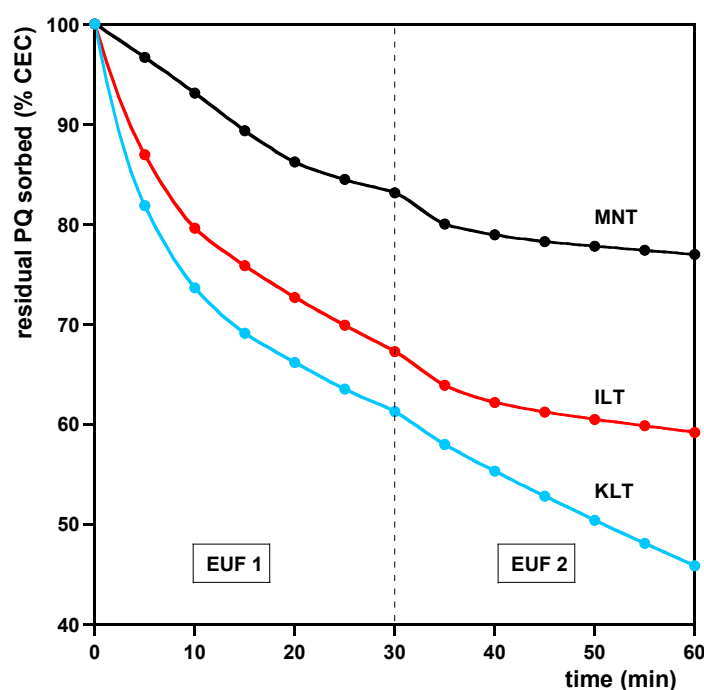
Figure 2. Residual PQ sorbed by the clays during the EUF stages, expressed as the percentage of residual PQ saturating the respective clay CECs.

The estimated R_m values corresponded to 65.1%, 42.2%, and only 24.2% of the CECs of KLN, ILT, and MNT, respectively. This suggests that montmorillonite exhibited a PQ replenishment ability with respect to its CEC substantially lower than those of kaolinite and illite. A similar trend was observed when PQ was added at the rates of 50 or 100 mg per g of clay (Table 3, Figure 3). However, the amounts of PQ retained by the MNT samples after 60 min of EUF extraction were dramatically larger than those retained by KLN or ILT. The comparative analysis of the R_m and k_1 parameters also showed that they both decreased in the order KLN > ILT > MNT, for both the PQ–50 and the PQ–100 treated samples, thus confirming the high buffer capacity of KLN and ILT for PQ and the strong PQ retention power of MNT.

Figure 4 shows the residual PQ retained after the EUF treatments by the differently cation-saturated MNT samples. It is evident that saturation with Ca^{2+} or Mg^{2+} resulted in a similar effect on EUF-PQ desorption, as shown by the extraction curves overlapping (Figure 4) in both EUF extraction runs. The cumulative EUF-PQ amounts extracted by

Ca-MNT and Mg-MNT were 21.36 and 21.62 mg g^{-1} after 30 min, and 24.9 and 25.0 mg g^{-1} after 60 min, respectively. Therefore, the PQ residual in the divalent-cation saturated clays satisfied 75% of the CEC. In contrast, the amounts of PQ extracted per gram of Na-MNT, K-MNT, and NH$_4$-MNT were 15.71, 18.20, and 16.47 mg g^{-1} after 30 min and 21.47, 24.75, and 24.01 mg g^{-1} after 60 min, so that the residual sorbed PQ was 77%, 75%, and 76% of the CEC, respectively. According to Table 4, the type of cation did not influence the maximum desorbable amount of PQ by MNT. However, the release rate of PQ was higher in the presence of divalent cations, as can be inferred from the values of k_1.
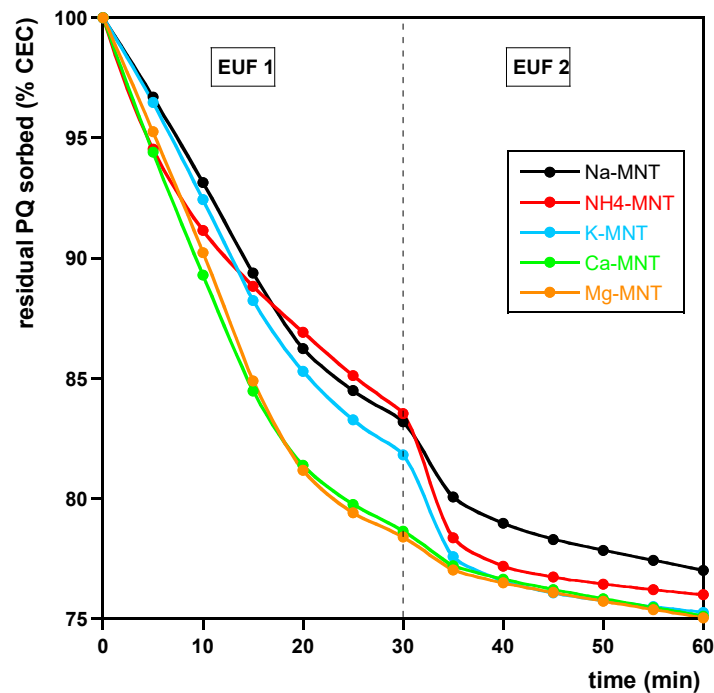
Table 3. Kinetic parameters for PQ desorption from Na clays during the EUF-2 stage, with PQ added in amounts corresponding to the respective clay CECs (EUF-PQCEC) or at the rate of 50 or 100 mg per g of clay (EUF-PQ50 or EUF-PQ100).

Model	R_m (%)	k_1 (min^{-1})	k_2 (min^{-1})	R^2
		KLN		
PFO (EUF-PQCEC)	65 ± 1	0.029 ± 0.001		0.9931
PSO (EUF-PQCEC)	91 ± 2		0.00027 ± 0.00002	0.9967
PFO (EUF-PQ50)	79.6 ± 0.2	0.072 ± 0.001		0.9906
PSO (EUF-PQ50)	87.6 ± 0.6		0.0068 ± 0.0004	0.9901
PFO (EUF-PQ100)	79.9 ± 0.1	0.074 ± 0.001		0.9947
PSO (EUF-PQ100)	87.4 ± 0.7		0.0018 ± 0.0001	0.9826
		ILT		
PFO (EUF-PQCEC)	42.2 ± 0.2	0.056 ± 0.001		0.9958
PSO (EUF-PQCEC)	50 ± 1		0.0016 ± 0.0001	0.9891
PFO (EUF-PQ50)	45.5 ± 0.1	0.069 ± 0.001		0.9955
PSO (EUF-PQ50)	50.6 ± 0.2		0.0104 ± 0.0004	0.9940
PFO (EUF-PQ100)	76.4 ± 0.1	0.15 ± 0.09		0.9782
PSO (EUF-PQ100)	81 ± 1		0.0034 ± 0.0006	0.9072
		MNT		
PFO (EUF-PQCEC)	24.2 ± 0.1	0.051 ± 0.001		0.9950
PSO (EUF-PQCEC)	29 ± 1		0.0022 ± 0.0002	0.9868
PFO (EUF-PQ50)	105.6 ± 0.2	0.099 ± 0.005		0.9995
PSO (EUF-PQ50)	110.4 ± 0.4		0.014 ± 0.001	0.9999
PFO (EUF-PQ100)	24.1 ± 0.1	0.051 ± 0.001		0.9950
PSO (EUF-PQ100)	29 ± 1	0.0022 ± 0.0002		0.9868
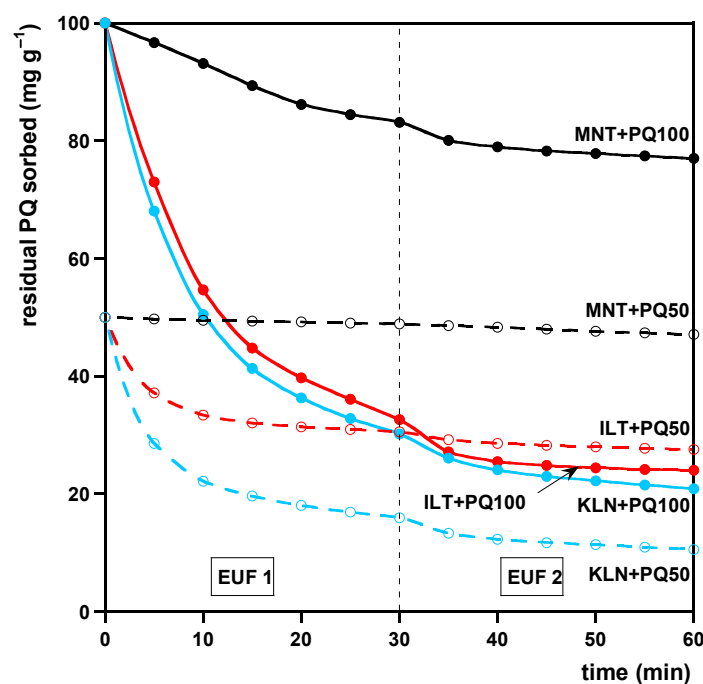
Figure 3. Residual PQ sorbed by the clay + PQ50 and clay + PQ100 samples during the EUF stages.

Figure 4. Residual PQ sorbed by MNT saturated with Na$^+$, K$^+$, NH$_4^+$, Ca^{2+}, and Mg^{2+}, expressed as the percentage of residual PQ saturating the respective clay CECs.

Table 4. Kinetic parameters for PQ desorption from MNT saturated with different cations during the EUF-2 stage.

Model	R_m (%)	k_1 (min^{-1})	k_2 (min^{-1})	R^2
		Na-MNT		
PFO (EUF-PQCEC)	24.1 ± 0.1	0.051 ± 0.001		0.9950
PSO (EUF-PQCEC)	29 ± 1		0.0022 ± 0.0002	0.9868
		K-MNT		
PFO (EUF-PQCEC)	25.3 ± 0.1	0.063 ± 0.002		0.9856
PSO (EUF-PQCEC)	29 ± 1		0.0036 ± 0.0005	0.9577
		NH4-MNT		
PFO (EUF-PQCEC)	24.7 ± 0.2	0.062 ± 0.003		0.9616
PSO (EUF-PQCEC)	28 ± 1		0.0036 ± 0.0007	0.9228
		Ca-MNT		
PFO (EUF-PQCEC)	25.2 ± 0.1	0.065 ± 0.002		0.9724
PSO (EUF-PQCEC)	28.4 ± 0.1		0.0040 ± 0.0002	0.9964
		Mg-MNT		
PFO (EUF-PQCEC)	25.3 ± 0.1	0.067 ± 0.002		0.9709
PSO (EUF-PQCEC)	28.3 ± 0.1		0.0044 ± 0.0002	0.9962

4. Discussion and Conclusions

The results of the sorption studies highlighted that PQ is much more effectively retained by montmorillonite than by kaolinite or illite. This is likely due to an interlayer sorption mechanism of PQ into expanding lattice clays such as montmorillonite [39]. Montmorillonite can trap PQ onto inner surfaces, taking away ions from the equilibrium solution, thus favoring further sorption. In our investigation, the XRD analyses showed that the basal d-spacing of Na-montmorillonite was 1.4 nm; after PQ addition, the d-spacing increased to 1.6 nm (see Figure 5). These data clearly confirmed that montmorillonite easily intercalates PQ; furthermore, according to the molecular structure of paraquat, we estimated the thickness of PQ ions to be about 0.2 nm, on the basis of the steric hindrance of the methyl

groups at C(6) and C(6′). In line with literature reports [40], it is then reasonable to infer that the bipyridinium moiety lies with aromatic rings parallel to the montmorillonite layers, probably together with some water molecules.
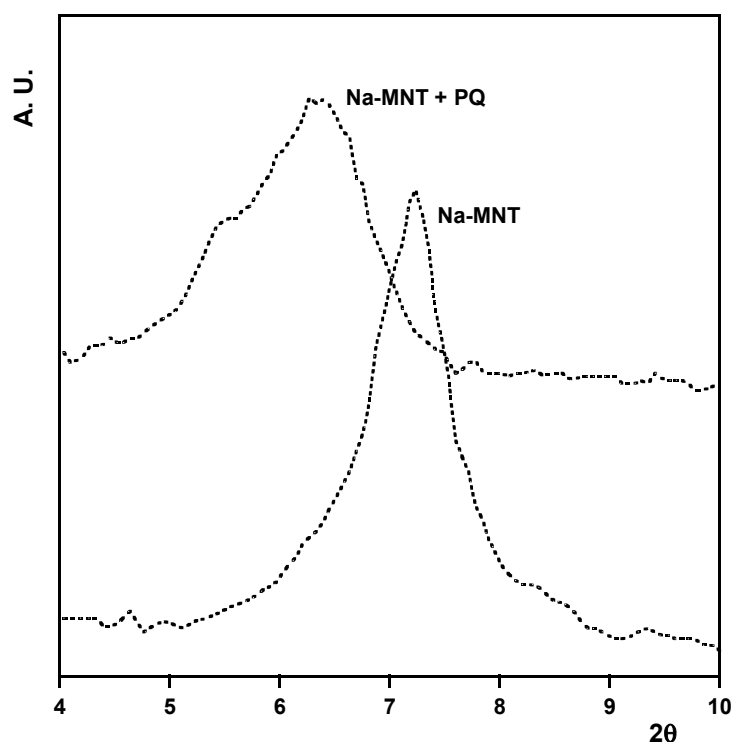
Figure 5. XRD spectra of Na-MNT with and without sorbed PQ.

The high affinity of PQ for montmorillonite would suggest that PQ held by this clay could be less extractable than that sorbed by kaolinite and illite; such a hypothesis is widely supported by our desorption studies, which clearly demonstrated that both the actual and the potential amounts of PQ extractable by EUF, as well as the desorption rate constants, decreased, following the order KLN > ILT > MNT. For MNT, the saturation with different cations induced some differences in the EUF-PQ desorption rate patterns, indicating that the presence of monovalent cations could further hamper paraquat release, while the opposite seems to be true for divalent cations. This finding could be related to the higher water coordination numbers of divalent cations compared to those of monovalent cations, which lead to a higher swelling degree of montmorillonite [41] and, hence, to an easier release of PQ.

The outcome of our study also revealed that the EUF technique may be a suitable tool for the quantitative and kinetic assessments of xenobiotic release from soil components.

Author Contributions: Software, S.S.; data curation, S.S.; writing—original draft preparation, S.S.; writing—review and editing, E.G. and E.C. All authors have read and agreed to the published version of the manuscript.

Abbreviations

PQ	Paraquat
KLN	Kaolinite
ILT	Illite
MNT	Montmorillonite
EUF	Electro–Ultrafiltration
EUF 1	First extraction step at low energy
EUF 2	Second extraction step at high energy
CEC	Cation-exchange capacity (cmol kg^{-1})
KLN + PQCEC	KLN containing an amount of PQ corresponding to its CEC value
ILT + PQCEC	ILT containing an amount of PQ corresponding to its CEC value
MNT + PQCEC	MNT containing an amount of PQ corresponding to its CEC value
KLN + PQ100	KLN containing an amount of PQ at a ratio of 10:1 (*w:w*)
ILT + PQ100	ILT containing an amount of PQ at a ratio of 10:1 (*w:w*)
MNT + PQ100	MNT containing an amount of PQ at a ratio of 10:1 (*w:w*)
KLN + PQ50	KLN containing an amount of PQ at a ratio of 20:1 (*w:w*)
ILT + PQ50	ILT containing an amount of PQ at a ratio of 20:1 (*w:w*)
MNT + PQ50	MNT containing an amount of PQ at a ratio of 20:1 (*w:w*)
Na-MNT	MNT saturated with Na^+ containing amounts of PQ corresponding to its CEC value
K-MNT	MNT saturated with K^+ containing amounts of PQ corresponding to its CEC value
NH4-MNT	MNT saturated with NH_4^+ containing amounts of PQ corresponding to its CEC value
Ca-MNT	MNT saturated with Ca^{2+} containing amounts of PQ corresponding to its CEC value
Mg-MNT	MNT saturated with Mg^{2+} containing amounts of PQ corresponding to its CEC value
q_e	Sorbed amount per mass of clay at equilibrium (mg g^{-1})
q_m	Maximum sorbable amount per mass of clay (mg g^{-1})
K_L	Equilibrium Langmuir constant (L mg^{-1})
K_F	Freundlich constant (L^N mg^{1-N} g^{-1})
N	Heterogeneity index of the Freundlich model (adimensional)
K_J	Jovanović constant (L mg^{-1})
PFO	Pseudo-first-order kinetic model
PSO	Pseudo-second-order kinetic model
S_t	Residual sorbed amount per mass of clay at time t
t	Extraction time
k_1	Kinetic rate constant related to the PFO kinetic model
k_2	Kinetic constants related to the EUF release rate of PQ
S_0	Initial content of releasable PQ
R_m	Maximum amount of releasable PQ per mass of clay

References

1. Syngenta Crop Protection. Available online: https://www.syngenta.com/en/protecting-crops/products-list/paraquat (accessed on 12 January 2024).
2. Wesseling, C.; Van Wendel De Joode, B.; Ruepert, C.; León, C.; Monge, P.; Hermosillo, H.; Partanen, L.J. Paraquat in Developing Countries. *Int. J. Occup. Environ. Health* **2001**, *7*, 275–286. [CrossRef]
3. Donaher, S.E.; Van den Hurk, P. Ecotoxicology of the herbicide paraquat: Effects on wildlife and knowledge gaps. *Ecotoxicology* **2023**, *32*, 1187–1199. [CrossRef]
4. Ardiwinata, A.N.; Harsanti, E.S.; Kurnia, A.; Sulaeman, E. The distribution of paraquat and carbosulfan residues in Indonesia. *IOP Conf. Ser. Earth Environ. Sci.* **2021**, *648*, 012033. [CrossRef]
5. Bromilow, R.H. Paraquat and sustainable agriculture. *Pest Manag. Sci.* **2004**, *60*, 340–349. [CrossRef]
6. Wang, H.; Pei, Z.; Chen, G.; Xing, B. Mutual influence of copper and paraquat on their adsorption in soil. *Pedosphere* **2023**, *33*, 857–864. [CrossRef]
7. Pateiro-Moure, M.; Arias-Estévez, M.; Simal-Gándara, J. Competitive and non-competitive adsorption/desorption of paraquat, diquat and difenzoquat in vineyard-devoted soils. *J. Hazard. Mater.* **2010**, *178*, 194–201. [CrossRef] [PubMed]
8. Salvestrini, S.; Canzano, S.; Iovino, P.; Leone, V.; Capasso, S. Modelling the biphasic sorption of simazine, imidacloprid, and boscalid in water/soil systems. *J. Environ. Sci. Health Part B Pestic. Food Contam. Agric. Wastes* **2014**, *49*, 578–590. [CrossRef] [PubMed]
9. Seki, Y.; Yurdakoç, K. Paraquat adsorption onto clays and organoclays from aqueous solution. *J. Colloid Interface Sci.* **2005**, *287*, 1–5. [CrossRef] [PubMed]

10. Spark, K.M.; Swift, R.S. Effect of soil composition and dissolved organic matter on pesticide sorption. *Sci. Total Environ.* **2002**, *298*, 147–161. [CrossRef] [PubMed]

11. Roberts, T.R.; Dyson, J.S.; Lane, M.C.G. Deactivation of the biological activity of paraquat in the soil environment: A review of long-term environmental fate. *J. Agric. Food Chem.* **2002**, *50*, 3623–3631. [CrossRef]

12. Weber, J.B.; Meek, R.C.; Weed, S.B. The Effect of Cation-Exchange Capacity on the Retention of Diquat2+ and Paraquat2+ by Three-Layer Type Clay Minerals: II. Plant Availability of Paraquat. *Soil Sci. Soc. Am. J.* **1969**, *33*, 382–385. [CrossRef]

13. Summers, L.A. *The Bipyridinium Herbicides*; Academic Press: London, UK; New York, NY, USA, 1980; p. 449.

14. Moyer, J.R.; Lindwall, C.W. Persistence and availability of paraquat in a Lethbridge clay loam soil. *Can. J. Soil Sci.* **1985**, *65*, 523–529. [CrossRef]

15. Tucker, B.V.; Pack, D.E.; Ospenson, J.N.; Omid, A.; Thomas, W.D. Paraquat Soil Bonding and Plant Response. *Weed Sci.* **1969**, *17*, 448–451. [CrossRef]

16. Boyd, N.S. Pepper and Tomato Root Uptake of Paraquat and Flumioxazin. *Weed Technol.* **2014**, *28*, 626–632. [CrossRef]

17. Ipor, I.B.; Price, C.E. Uptake, translocation and activity of paraquat on Mikania micrantha H.B.K. grown in different light conditions. *Int. J. Pest Manag.* **1994**, *40*, 40–45. [CrossRef]

18. Hart, J.J.; Di Tomaso, J.M.; Linscott, D.L.; Kochian, L.V. Characterization of the transport and cellular compartmentation of paraquat in roots of intact maize seedlings. *Pestic. Biochem. Physiol.* **1992**, *43*, 212–222. [CrossRef]

19. DiTomaso, J.M.; Hart, J.J.; Kochian, L.V. Compartmentation Analysis of Paraquat Fluxes in Maize Roots as a Means of Estimating the Rate of Vacuolar Accumulation and Translocation to Shoots. *Plant Physiol.* **1993**, *102*, 467–472. [CrossRef]

20. Cheah, U.B.; Kirkwood, R.C.; Lum, K.Y. Adsorption, desorption and mobility of four commonly used pesticides in Malaysian agricultural soils. *Pestic. Sci.* **1997**, *50*, 53–63. [CrossRef]

21. Kumar, J.; Nisar, K.; Shakil, N.A.; Walia, S.; Parsad, R. Controlled release formulations of metribuzin: Release kinetics in water and soil. *J. Environ. Sci. Health Part B* **2010**, *45*, 330–335. [CrossRef] [PubMed]

22. Salvestrini, S.; Vanore, P.; Iovino, P.; Leone, V.; Capasso, S. Adsorption of simazine and boscalid onto acid-activated natural clinoptilolite. *Environ. Eng. Manag. J.* **2015**, *14*, 1705–1712. [CrossRef]

23. Németh, K. The availability of nutrients in the soil as determined by electro-ultrafiltration (EUF). *Adv. Agron.* **1980**, *31*, 155–188. [CrossRef]

24. Sager, M. Modelling the Plant Uptake of Metals from Release Rates Obtained by the EUF Method. *Plants* **2021**, *11*, 85. [CrossRef]

25. Chen, G.; Song, W.; Qi, B.; Lu, J.; Wan, Y. Recycling cellulase from enzymatic hydrolyzate of acid treated wheat straw by electroultrafiltration. *Bioresour. Technol.* **2013**, *144*, 186–193. [CrossRef] [PubMed]

26. Fu, C.; Yi, X.; Gao, Y. Effect of Electric Field on Membrane Fouling and Membrane Performance in Reverse Osmosis Treatment of Brackish Water. *Appl. Sci.* **2024**, *14*, 575. [CrossRef]

27. Mohammad, A.W.; Ng, C.Y.; Lim, Y.P.; Ng, G.H. Ultrafiltration in Food Processing Industry: Review on Application, Membrane Fouling, and Fouling Control. *Food Bioprocess Technol.* **2012**, *5*, 1143–1156. [CrossRef]

28. Li, M.; Zuo, K.; Liang, S.; Xiao, K.; Liang, P.; Wang, X.; Huang, X. Electrically Tuning Ultrafiltration Behavior for Efficient Water Purification. *Environ. Sci. Technol.* **2020**, *54*, 11536–11545. [CrossRef] [PubMed]

29. Buondonno, A.; Felleca, D.; Bufo, S.A.; Pizzigallo, M.D.R.; Testini, C. Comparison between electro-ultrafiltration and extraction methods for the determination of k fractions in some soils of southern Italy. *Commun. Soil Sci. Plant Anal.* **1988**, *19*, 239–258. [CrossRef]

30. Jelecevic, A.; Horn, D.; Eigner, H.; Sager, M.; Liebhard, P.; Moder, K.; Vollprecht, D. Kinetics of lead release from soils at historic mining and smelting sites, determined by a modified electro-ultrafiltration. *Plant Soil Environ.* **2019**, *65*, 298–306. [CrossRef]

31. Varga, I.; Jović, J.; Rastija, M.; Markulj Kulundžić, A.; Zebec, V.; Lončarić, Z.; Iljkić, D.; Antunović, M. Efficiency and Management of Nitrogen Fertilization in Sugar Beet as Spring Crop: A Review. *Nitrogen* **2022**, *3*, 170–185. [CrossRef]

32. Postolache, S.; Sebastião, P.; Viegas, V.; Postolache, O.; Cercas, F. IoT-Based Systems for Soil Nutrients Assessment in Horticulture. *Sensors* **2022**, *23*, 403. [CrossRef]

33. Langmuir, I. The adsorption of gases on plane surfaces of glass, mica and platinum. *J. Am. Chem. Soc.* **1918**, *40*, 1361–1403. [CrossRef]

34. Freundlich, H. Über die Adsorption in Lösungen. *Z. Phys. Chem.* **1907**, *57U*, 385–470. [CrossRef]

35. Jovanović, D.S. Physical adsorption of gases—I: Isotherms for monolayer and multilayer adsorption. *Kolloid-Z. Z. Polym.* **1969**, *235*, 1203–1213. [CrossRef]

36. Chu, K.H.; Hashim, M.A.; Debord, J.; Harel, M.; Salvestrini, S.; Bollinger, J.C. The Jovanović adsorption isotherm in water contaminant research: Unmasking spurious versions and spotlighting the real thing. *Chem. Eng. Sci.* **2023**, *281*, 119127. [CrossRef]

37. Salvestrini, S. A modification of the Langmuir rate equation for diffusion-controlled adsorption kinetics. *React. Kinet. Mech. Catal.* **2019**, *128*, 571–586. [CrossRef]

38. Debord, J.; Chu, K.H.; Harel, M.; Salvestrini, S.; Bollinger, J.C. Yesterday, Today, and Tomorrow. Evolution of a Sleeping Beauty: The Freundlich Isotherm. *Langmuir* **2023**, *39*, 3062–3071. [CrossRef] [PubMed]

39. Ilari, R.; Etcheverry, M.; Waiman, C.V.; Zanini, G.P. A simple cation exchange model to assess the competitive adsorption between the herbicide paraquat and the biocide benzalkonium chloride on montmorillonite. *Colloids Surf. A Physicochem. Eng. Asp.* **2021**, *611*, 125797. [CrossRef]

40.   Wang, M.; Orr, A.A.; He, S.; Dalaijamts, C.; Chiu, W.A.; Tamamis, P.; Phillips, T.D. Montmorillonites Can Tightly Bind Glyphosate and Paraquat Reducing Toxin Exposures and Toxicity. *ACS Omega* **2019**, *4*, 17702–17713. [CrossRef] [PubMed]

41.   Yotsuji, K.; Tachi, Y.; Sakuma, H.; Kawamura, K. Effect of interlayer cations on montmorillonite swelling: Comparison between molecular dynamic simulations and experiments. *Appl. Clay Sci.* **2021**, *204*, 106034. [CrossRef]